

## FEDSM-ICNMM2010-30+\$+

### EXPERIMENTAL INVESTIGATION OF AERIAL SPRAY CHARACTERISTICS

**Ali Bagherpour**

Department of Mechanical Engineering  
University of New Brunswick  
15 Dineen Drive, Fredericton  
Canada  
t2elf@unb.ca

**Gordon Holloway\***

Department of Mechanical Engineering  
University of New Brunswick  
15 Dineen Drive, Fredericton, NB  
Canada  
Holloway@unb.ca

**Ian M. McLeod**

Forest Protection Limited  
Fredericton, NB  
Canada  
IMcLeod@ForestProtectionLimited.com

#### ABSTRACT

*An important characteristic of sprays is their statistical distribution of droplet sizes. Knowledge of the droplet distribution is particularly important for pesticide applications because droplet size affects droplet trajectory, probability of contact with foliage, and the biological dose to target pests. This work describes an experimental study of an aerial spray application in a wind tunnel environment at realistic flight speeds (67 m/s) using a full-scale rotary atomizer turning at 8600 rpm. Comparative measurements of water droplet velocity and diameter were made a 3 component Artium Phase Doppler Interferometer (PDI) and a Sympatec Helos Vario Laser Diffraction (LD) instrument. Distance from the atomizer to the measurement cross section was varied to observe the effects of the atomizer wake on the results.*

#### NOMENCLATURE

$D$  Atomizer blade diameter  
 $F$  Cumulative probability density function  
 $F_v$  Volumetric cumulative probability density function  
 $N$  Number of droplets  
 $R$  Rejection rate  
 $T$  Measurement time interval  
 $U$  Gas-phase velocity in x direction  
 $d_{v0.1}$  Drop diameter such that 10% of the total liquid volume is in drops of smaller diameter [1]  
 $d_{v0.5}$  Volume Median Diameter (VMD)

$d_{v0.9}$  Drop diameter such that 90% of the total liquid volume is in drops of smaller diameter [1]  
 $f$  Probability density function  
 $f_v$  Volumetric probability density function  
 $r$  Radius  
 $x$  Distance downstream of the atomizer along the tunnel  
 $u$  Droplet velocity in x direction  
 $\Lambda$  Droplet Number Concentration ( $\#/m^3$ )  
 $\Lambda_v$  Volume Concentration ( $m^3/m^3$ )  
 $\Phi$  Droplet number flux ( $\#/m^2/s$ )  
 $\Phi_v$  Volume flux ( $m^3/m^2/s$ )  
 $\lambda$  Droplet number rate

#### INTRODUCTION

Rotary atomizers are widely used in aerial spray applications. An important characteristic of rotary atomizers is their statistical distribution of droplet sizes. Knowledge of the size distribution of the droplet produced by a sprayer is particularly important for pesticide applications because droplet size affects droplet trajectory (drift), probability of contact with foliage, and the biological dose to target pests.

MicronAir AU4000 atomizer is a rotary atomizer that has been used widely in the aerial spraying. This atomizer produce a narrow spectrum of droplet sizes at the operating airspeed of 23-88 m/s [2]. There are various studies on characterizing the droplet size distribution of MicronAir AU4000 and other rotary cage atomizers [3–7]. These studies show that the droplet size

\*Address all correspondence to this author.

spectra of the rotary atomizers is a function of airstream velocity, liquid flow rate, liquid properties such as viscosity and surface tension.

Two common optical systems used to evaluate the droplet size spectrum of the rotary atomizers are Laser Diffraction (LD) and Phase Doppler Interferometer (PDI) systems [7–12]. LD measures the size distribution of a cloud of droplets in a finite volume (spatial or concentration-based sampling [1]). LD has a high sampling rate and therefore requires short times to gather data. Light is scattered by all droplets in the beam at a given instant and multiple photo detectors measure the aggregate forward scattering pattern. A deconvolution method is used to calculate the size distribution of the sample. However LD does not provide droplet velocity information and therefore cannot be used alone to estimate droplet flow rates or flux.

The other widely used droplet sizing system is Phase Doppler Interferometer. PDI is an optical and non-intrusive instrument suitable for measuring local mass flux of liquid sprays [13]. This method provides the size and velocity of the droplets passing through a small probe volume in a time interval (temporal or flux-sensitive sampling [1]). In recent years PDI has been used in various applications including cloud physics [14], fire suppression [15], spray and atomization applications [16,17] and others, in order to measure the velocity, size distribution and volume flux of the droplets in the sprays. It is important to note that it is the droplet size spectra based on temporal sampling that is of direct relevance to aerial spray applications and this is an inherent advantage of PDI instrument.

It has been shown that LD and PDI systems produce different droplet size distributions under similar test conditions [12]. Dodge [8] reviewed a comprehensive study of droplet sizing for many hydraulic sprayers, at different laboratories, using several instrument types including PDI and LD. Young and Bachalo [18] investigated the difference between the results of temporal (PDI & PMS: Particle Measuring System) and spatial (LD) sampling for the hydraulic sprays. They proposed an approximate method to transform the results of these sampling methods from one to the other. To apply this transform the velocity of the droplets must be measured in each size class.

In this work the size distribution of the droplets produced by a MicronAir AU4000 atomizer is measured using PDI and LD systems to form a comparison. These systems measure different quantities and have errors and uncertainties but they should give similar result for droplet size spectra in spatially uniform sprays with uniform velocity fields. However such ideal conditions are often unavailable and interpretation of LD results can become uncertain in cases where there exists a strong velocity gradient or significant spatial segregation of droplets by size. For rotary atomizer sprays typical of aerial spraying, both of these problematic issues are prominent in the near-wake where measurements are often made. This paper presents the size distribution of droplets measured by both systems at different distances down-

stream of a MicronAir AU4000 atomizer. At various distances downwind of the sprayer some sources of errors and difference between the size distributions are discussed.

## EXPERIMENTAL APPARATUS

The experimental apparatus used to study a full scale AU4000 atomizer consists of a wind tunnel facility that has available a suite of instruments that includes: a Sympatec Helos Vario laser diffraction system, a 3-component Artium Technologies Phase Doppler Interferometer, hot-wire anemometry, high-speed stroboscopic imaging and stroboscopic particle image velocimetry.

### Wind Tunnel

The test section of the wind tunnel is 1 m in diameter and 5 m in length. All droplet measurements are taken through an optical access port at the end of the test section, Fig. 1. The air velocity ranges from 10 m/s up to 85 m/s in the test section. The unobstructed tunnel airstream is highly uniform and has a turbulence level of less than 1%. Full-scale atomizers are attached to

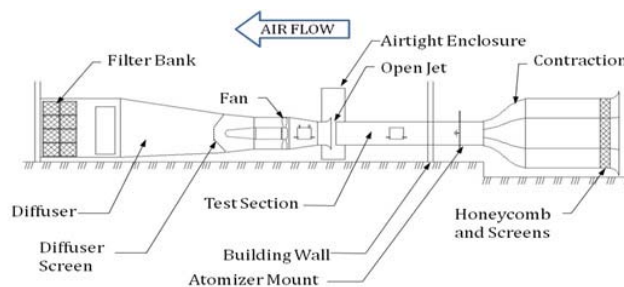


FIGURE 1. SCHEMATIC OF WIND TUNNEL FACILITY

a boom on the tunnel centerline and linked to the fluid supply and measurement system. The atomizer position relative to the measurement location can be adjusted between 0.15 m and 4.5 m. Fluid is supplied to the atomizer by a rotary-vane positive displacement pump and its flow rate is measured by a precision turbine flow meter.

### Stroboscopic Imaging

This technique employs a high-frame rate CMOS camera (up to 1000 frames/second) whose shutter is synchronized with a stroboscopic floodlight for illumination of the subject. The high frame rate allows qualitative examination of the very near-wake of the atomizer. Qualitative knowledge of the length and shape of the near-wake region is very useful in interpretation of measurements and development of computational models of the spray.

High-speed imagery also allows examination of atomizer geometries and construction, such as turbine blades and weld seams, and their influence on production of droplets. A spray image is shown in Figure 4.

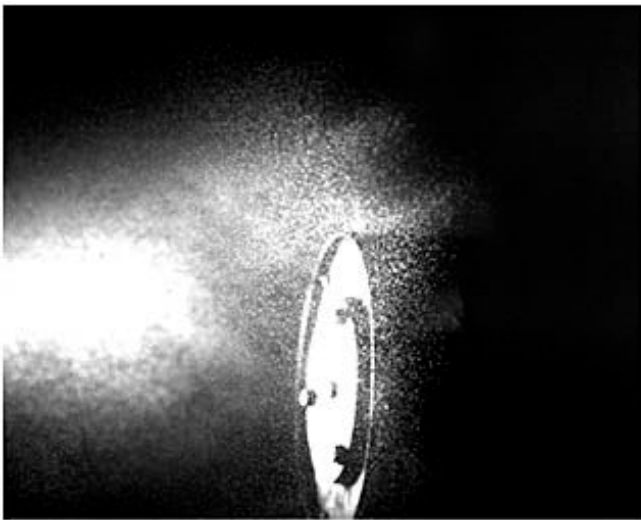


**FIGURE 2.** STROBOSCOPIC IMAGES OF SPRAY FROM AN AU4000 AT 10 *l/min*, 1100 *rpm*, AND 75 *m/s* AIR SPEED.

### Hotwire Anemometry

Air velocity in the absence of droplets, but with the atomizer present and spinning, was measured using hotwire anemometry techniques. Hotwire probes respond quickly to changes in velocity and are suited to quantify fluctuations in high-turbulence flows such as the near-wake of the atomizer. For the tests a hotwire probe (DISA 55P01) with a Dantec 56C17 constant-temperature anemometer (CTA) was used. In spite of the high turbulence levels measured in the near wake of the atomizer no instantaneous flow reversals were observed.

### Laser Diffraction (LD)

The Sympatec Helos Vario estimates the droplet size spectrum and concentrations based on the principles of Fraunhofer scattering theory [19]. The system employs a laser transmitter that directs a 5 *mW* red (632.8 *nm*) laser beam across the spray plume. The default beam diameter which is 26 *mm* was used in these experiments. Light is scattered by droplets to varying degrees based on droplet size. A receiver with the distance of 1.2 *m* at the opposite side of the plume contains detecting elements that measure the amount of light scattering and the pattern it creates. The R6 lens was used in the receiver. The diffraction pattern of the droplets within the beam determined by sensor information

is interpreted to produce a size distribution for the droplets. LD also provides a measure of the beam obscuration, or extinction, in the droplet field. Obscuration is displayed as a percentage of the initial beam intensity and represents the fraction of light scattered by the droplets. The obscuration data is used to estimate the number of droplets in the beam.

### Phase Doppler Interferometry (PDI)

The PDI simultaneously measures size and velocity of droplets passing through a small volume of space - the crossing point of two laser beams using the principles of light scattering by refraction [20, 21]. Results at the point of interest are unaffected by any intervening droplets on the transmitter or the receiver sides of the crossing and spatial segregation or velocity non-uniformity. In this set of experiments the Artium Technologies PDI300 is used. PDI300 is capable of measuring droplet size and 3-components of velocity. Two transmitters units produce two pairs of green (532 *nm*) and one pair of blue (473 *nm*) laser beams. The beam spacing was 60 *mm* for all the transmitters and The receiver unit houses 3 light detectors to collect refracted light at a forward angle of 20°. 1 *m* focal length lenses are used for both the transmitters and the receiver.

Particle velocity measurement made available by PDI provides the opportunity to estimate spatial samples (as in the case of LD) for each size class of droplet.

## RESULTS

Measurements were made for the spray plume produced by a MicronAir AU4000 turbine-driven rotary atomizer using a blade angle of approximately 35° with the EX2665 blade kit, a rotational speed of 8600 *rpm* (measured with a strobe light with fluid flow) at a wind speed of 67 *m/s*. Water was supplied to the atomizer at a rate of 4 *L/min*. These conditions were selected to simulate a typical aerial application configuration. Measurements of the spray plume were made at distances of 0.5, 1.0, 2.0 and 4.0 *m* downstream of the atomizer. The atomizer remains centered in the tunnel cross section for all tests to minimize unwanted interference by the wind tunnel walls.

### LD Experiments

Each measurement of a given plume consists of a series of transects of the LD beam across the spray plume cross section, see Fig. 3. The LD beam was traversed vertically across the plume while the atomizer and plume position are fixed within the tunnel. The results of each transect produce separate size distribution that can be aggregated into size distribution of the entire plume (calculated using obscuration weighting of each transect). Measurements were made at 2 *cm* intervals over the height of the tunnel with the duration of each measurement being 3 seconds. The maximum sampling rate of 2000 *Hz* was used to produce

6000 instantaneous samples for each transect. The LD requires a reference measurement that records the sensor values when no spray droplets are present to account for extinction created by lens fogging, dust particles and viewport surface inconsistency. The present measurement procedure includes a reference measurement for each transect to eliminate the effect glass non-uniformity on the measurements. A time delay was incorporated between reference and measurement phases of the LD to allow time for the spray plume to fully develop after activation.

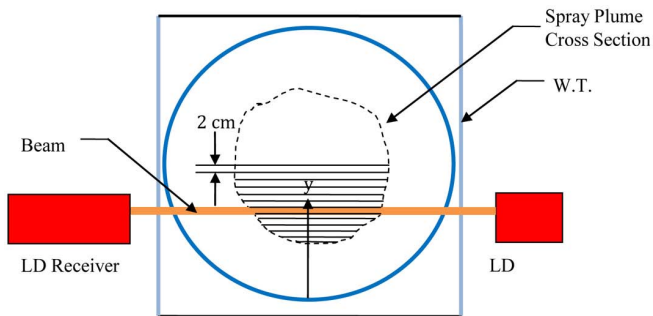


**FIGURE 3.** TRAVERSING METHOD FOR LD MEASUREMENTS. EACH TRANSECT REPRESENTS A PHYSICAL "CHORDLINE" OF THE SPRAY PLUME CROSS SECTION.

For LD measurements obscuration is defined as

$$Ob = 1 - I_r / I_t \quad (1)$$

where  $I_r$  is the light intensity measured by the LD receiver after passing through the spray plume and  $I_t$  is the light intensity leaving the transmitter. Figure 4 shows the obscuration and  $d_{v0.5}$  (Volume Median Diameter) for each transect across the spray plume for each downstream distances. This shows that the droplets are strongly segregated spatially according to size with the largest droplets at the outer edge of the plume and this persists to  $x = 4.0 m$ . It should be noted that the obscuration is relatively high in the near wake at the center of the tunnel increasing the probability of multiple scattering.

Distribution characteristics:  $d_{v0.1}$ ,  $d_{v0.5}$  and  $d_{v0.9}$  for the entire plume and the centerline transect of the plume at each streamwise measurement position are shown in Fig. 5. This shows a general trend of measuring values for  $d_{v0.5}$  and  $d_{v0.9}$  with the centerline transect values consistently less than the plume average results. Measurements made in the near wake,  $x < 0.5 m$ , gives significantly lower values.

The volumetric probability density function,  $f_v(d)$ , is re-

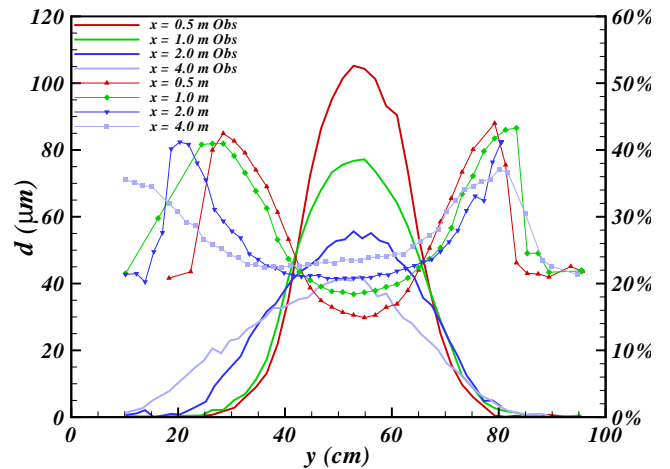


**FIGURE 4.** OBSCURATION AND  $d_{v0.5}$  (VMD) PROFILES FOR TRANSECTS ACROSS THE SPRAY PLUME AS DETERMINED BY LD.

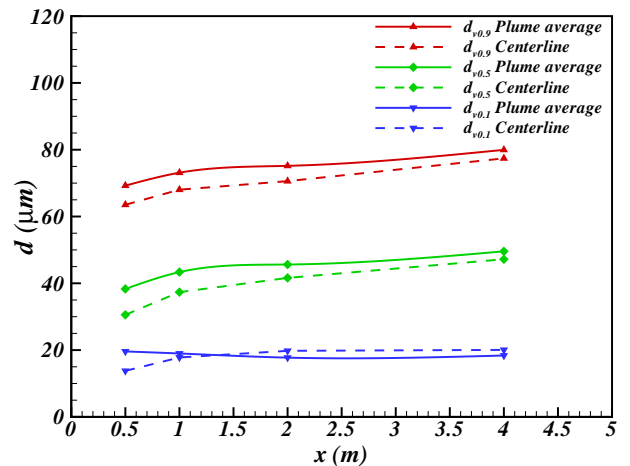


**FIGURE 5.** DEVELOPMENT OF  $d_{v0.1}$ ,  $d_{v0.5}$ , AND  $d_{v0.9}$  WITH DOWNSTREAM DISTANCE FROM THE ATOMIZER AS DETERMINED BY LD. PLUME AVERAGE RESULTS WERE CALCULATED BY OBSCURATION WEIGHTING OF EACH TRANSECT.

lated to the cumulative volume distribution,  $F_v(d)$ , as

$$f_v(d) = \frac{dF_v(d)}{dd} \quad (2)$$

Figures 6&7 show  $f_v(d)$  and  $F_v(d)$  for the obscuration weighted plume average and centerline transect results. There is clearly a greater contribution of small droplets to the plume average results at  $x = 0.5 m$  than at  $x = 4.0 m$  distribution.

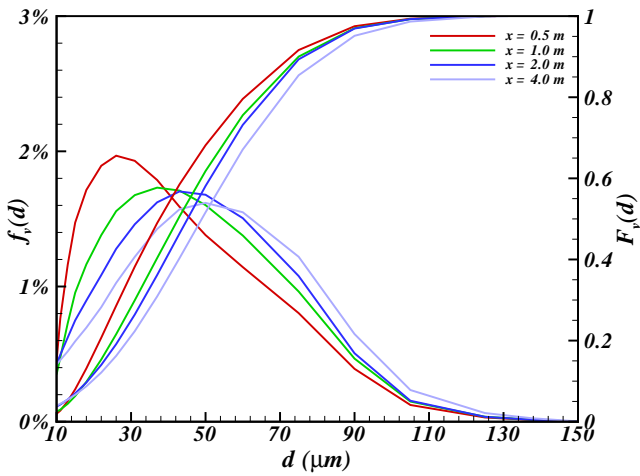


**FIGURE 6.** PLUME AVERAGE VOLUMETRIC PDF'S AT DISTANCES DOWNSTREAM FROM THE ATOMIZER

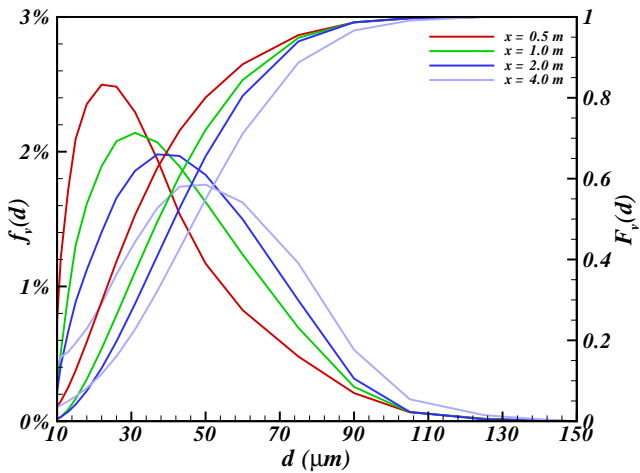


**FIGURE 7.** CENTERLINES TRANSECT VOLUMETRIC PDF'S AT DISTANCES DOWNSTREAM FROM THE ATOMIZER.

### PDI Experiments

Measurements of droplet size and velocity were made along a horizontal radial lines at measurement stations:  $x = 0.5, 1.0, 2.0$  and  $4.0$  m. Figure 8 shows the scanning pattern for each test. At each radial position either 200,000 droplets were measured or data was gathered for 300 seconds; whichever occurred first.

The data rate at each point is defined as,  $\lambda = N/T$ , in which  $N$  is the number of detected droplets in the measurement time interval,  $T$ , which varied from 13 s to 300 s. Figure 9 shows the measured data rate profile across the plume for different positions downstream of the sprayer. The data rate in the range  $2r/D < 2$  ( $D = 22.9$  cm is the diameter of the atomizer) was high enough to result in multiple droplets being present in the measurement

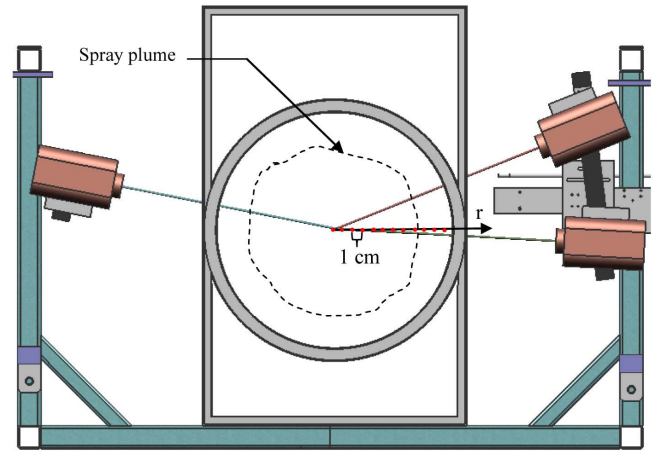


**FIGURE 8.** PDI SETUP AND SCANNING PATTERN.

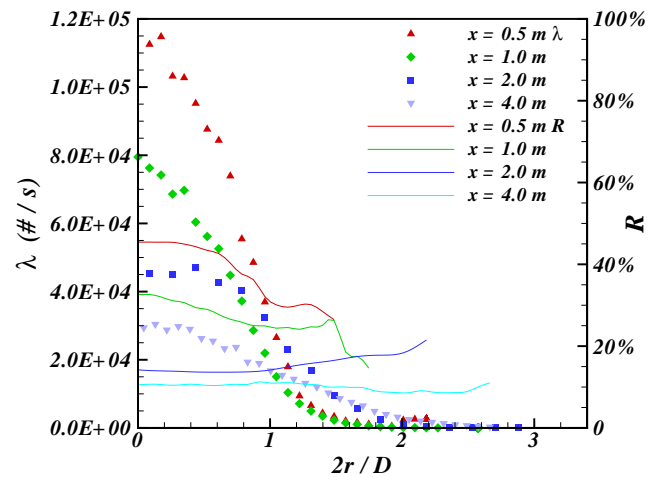


**FIGURE 9.** PROFILES OF MEASURED DATA RATE AND REJECTION RATE,  $R$ , ALONG A RADIAL LINE ACROSS THE PLUME AT VARIOUS STREAMWISE POSITIONS. DATA SHOWN HAS BEEN CORRECTED FOR REJECTIONS.

volume as much as 40% of the time. When this occurred the signal was "rejected". The profiles of the rejection rate,  $R$ , are shown in Fig. 9. Corrected data rates based on the assumptions that the temporal distribution is Poisson and that the "accepted" data (where only 1 droplet was present in the measurement volume) is an unbiased sample have been applied to the data shown in Fig. 9 [22].

The PDI has the capability to simultaneously measure the droplet size,  $d$ , and streamwise component of velocity,  $u$ , and therefore the joint probability density functions of these two variables,  $f(d, u)$ . The marginal statistics of velocity or diameter,  $f(d)$  and  $f(u)$ , may be calculated from the joint probability den-

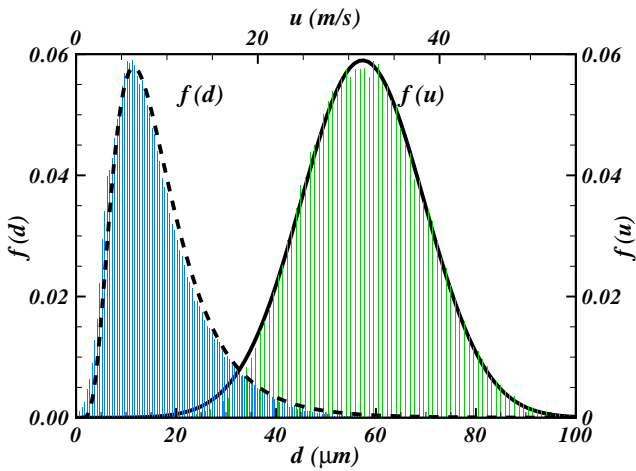


**FIGURE 10.** DROPLET SIZE AND VELOCITY PROBABILITY FUNCTIONS AT  $x=0.5\text{ m}$ ,  $r=0\text{ cm}$ . DASHED AND SOLID LINES REPRESENT A LOG-NORMAL AND NORMAL DISTRIBUTION.

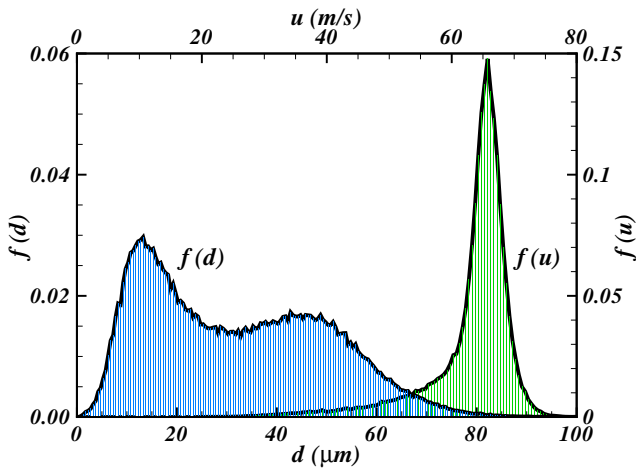


**FIGURE 11.** DROPLET SIZE AND VELOCITY PROBABILITY FUNCTIONS AT  $x=0.5\text{ m}$ ,  $r=12\text{ cm}$ .

sity function as shown in Fig. 10 for  $r=0\text{ cm}$  and Figs. 11 for  $r=12\text{ cm}$ . On the plume center  $f(d)$  is nearly log normal and  $f(u)$  is nearly normal as indicated by the dashed line. However at  $r=12\text{ cm}$ ,  $f(d)$  is clearly bimodal as it represents a mixture of large and small droplet distributions. The presence of these large droplets is also detected by LD in the transects on the spray fringe shown in Fig. 4 and they should also contribute to the centerline transect.

The air velocity, or gas phase in the presence of spray, were inferred from the velocity of the small droplets ( $d < 8\mu\text{m}$ ) that are measured with the PDI. The radial profiles of the mean streamwise component of the gas phase velocity,  $U$ , at differ-

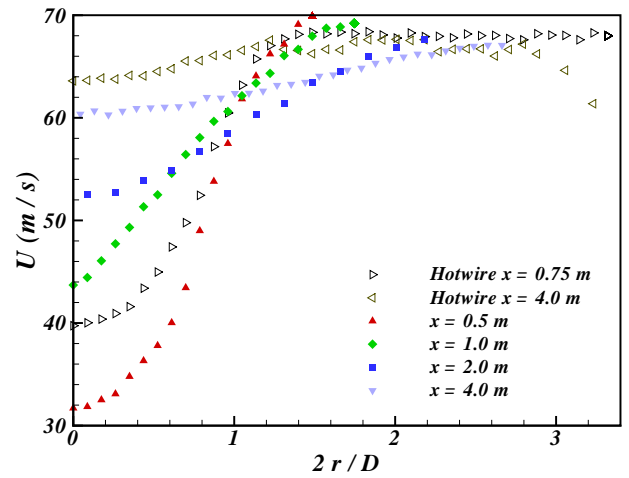


**FIGURE 12.** GAS PHASE MEAN VELOCITY PROFILES INFERRED FROM SMALL DROPLET VELOCITIES ( $d < 8\mu\text{m}$ ).

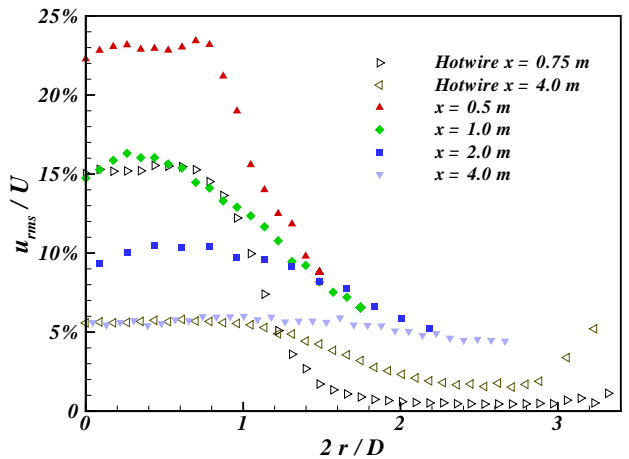


**FIGURE 13.** TURBULENCE INTENSITY PROFILES INFERRED FROM SMALL DROPLET VELOCITIES ( $d < 8\mu\text{m}$ ).

ent streamwise positions are shown in Fig. 12. Also shown are profiles taken using a hot wire anemometer with the rotating atomizer in place, spinning, but without liquid flow. In the near wake  $U$  is 50% lower than the free stream velocity while at  $x=4\text{ m}$  the velocity profile has become more uniform with a velocity difference across the plume of less than 10%. The hotwire velocity profiles show a similar trend and are surprisingly close to the flow loaded with droplets. Profiles of turbulence intensity of the gas phase velocity are shown in Fig. 13. As expected at  $x=0.5\text{ m}$  the turbulence intensity is very high,  $u_{rms}/U = 23\%$ , but is reduced to 5% at  $x=4\text{ m}$ . In the near wake and on the edge of the spray the hot wire results suggest that the droplets play a significant role in enhancing the turbulence.

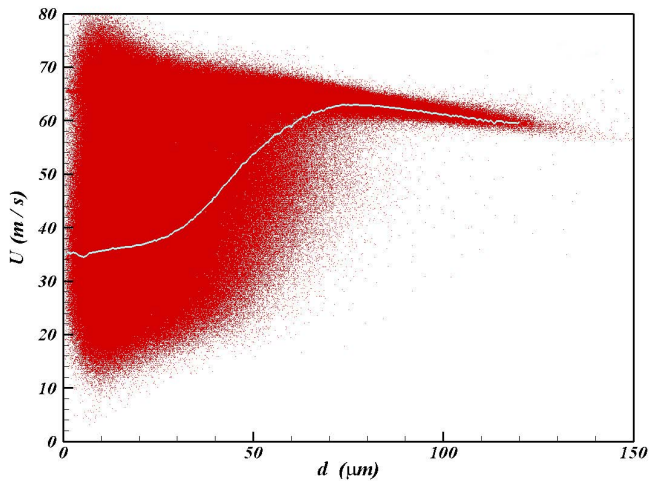


**FIGURE 14.** AGGREGATED PDI DATA FOR THE CENTERLINE TRANSECT AT  $x = 0.5 \text{ m}$ . EACH RED DOT INDICATES A DATA POINT AND THE LIGHT BLUE LINE IS THE MEAN CORRELATION LINE.

It is also possible to derive from the PDI data aggregate statistics for data gathered from all radial positions at a given streamwise position  $x$ . This would correspond to a centerline transect sample which is more representative of the plume than any one position. The velocity and diameter of each droplet sampled at  $x = 0.5 \text{ m}$  is shown in Fig. 14 including a line of mean correlation between the droplet velocity and diameter. There is a large amount of scatter about this mean line but one can still conclude that a significant correlation exists between droplet velocity and diameter for the aggregate data. This correlation is not present in *jpdfs* of data from single points and therefore must result from the spatial segregation of droplets according to size and velocity. Mean correlations lines at other streamwise positions are shown in Fig. 15 and it can be seen that the correlation between droplet velocity and size is greatly diminished by  $x = 4 \text{ m}$ .

## COMPARISON BETWEEN LD AND PDI MEASUREMENTS

As described in the previous section the PDI uses a time record of droplets passing through a small probe volume one at a time and its sampling is generally referred to a flux-sensitive [1] as opposed to the concentration-based sampling of LD. However it has been shown [18] that an approximate transform can be made from the temporal data sample to a spatial data sample using the mean velocity of the droplets of each size class at each position. The transform,  $\Lambda_i = \Phi_i / U_i$ , where  $\Lambda_i$  is the droplet number concentration per unit volume for size class  $i$  and  $\Phi_i$  is the droplet number flux per unit area per unit time.  $U_i$  is the

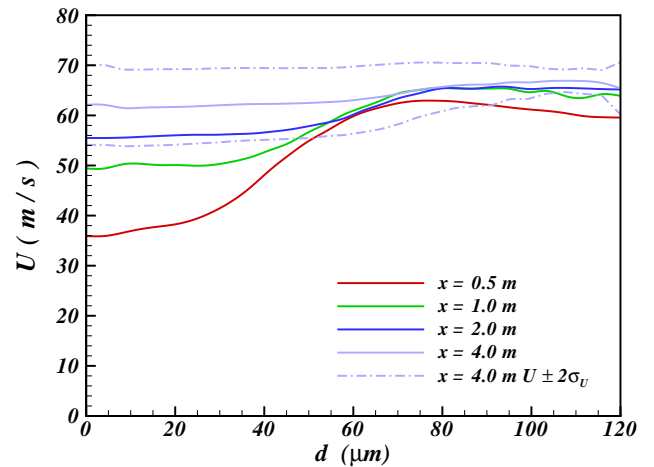


**FIGURE 15.** MEAN CORRELATION LINES FOR AGGREGATED PDI DATA CORRESPONDING TO THE CENTERLINE TRANSECT AT VARIOUS STREAMWISE POSITIONS. DASHED LINES SHOW  $u \pm 2\sigma_u$  AT  $x = 4.0 \text{ m}$ .

mean velocity of the size class according to Figs. 10&11. Figures 16&17 show profiles of the droplet number flux,  $\Phi = \sum_i \Phi_i$ , obtained using the PDI and the droplet number concentration,  $\Lambda = \sum_i \Lambda_i$ , obtained from the PDI data using the transformation above. In effect, droplets moving at low mean velocity in the near wake results in a high concentration of small droplets in this region that contribute less to the flux than the mean velocity of the flow would suggest. Also shown are the radial profiles of droplet volume flux,  $\Phi_v$ , and droplet volume concentration,  $\Lambda_v$ . Note that in the near wake the large droplets on the periphery of the spray make a very large contribution to the droplet volume statistics.

A direct comparison between the PDI and LD measurements can be made using PDI data aggregated from the measurement positions distributed along the radial line. Figure 18 shows the result for temporal samples of the data and Fig. 19 shows the result for spatial samples as obtained by transformation from the PDI data using the size class velocity data of Fig. 15. The volumetric *pdf*'s at  $x = 0.5 \text{ m}$  and  $1.0 \text{ m}$  show a significant volume of large droplets that is significantly diminished at greater downstream distances. These large droplets were observed at the edge of the spray where they have a high velocity, see Figs. 14. Comparing Figs. 18&19 we can see the transformation from temporal to spatial sampling has a strong effect on the small droplet range at positions of  $x = 0.5$  and  $1.0 \text{ m}$  where small droplets are highly concentrated in the near wake but moving at low velocity, see Fig. 17. At  $x = 4.0 \text{ m}$ , the transformation has a small effect - as one might expect - since the spray droplet sizes and their velocities are more uniformly distributed in space.

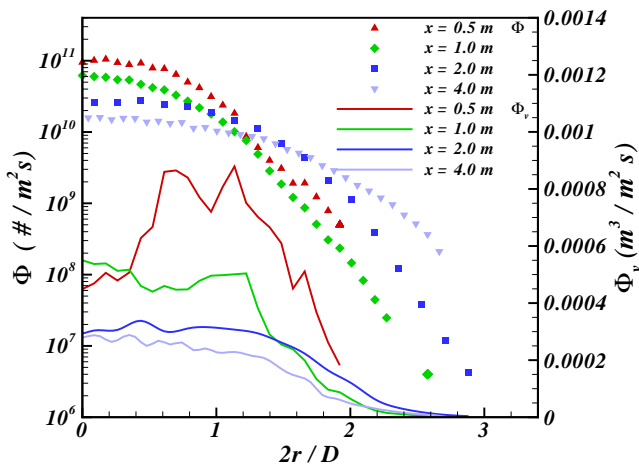


**FIGURE 16.** RADIAL PROFILE OF NUMBER FLUX,  $\Phi$ , REPRESENTED BY SYMBOLS AND VOLUME FLUX,  $\Phi_v$ , REPRESENTED BY SOLID LINES FOR VARIOUS DOWNSTREAM POSITIONS.

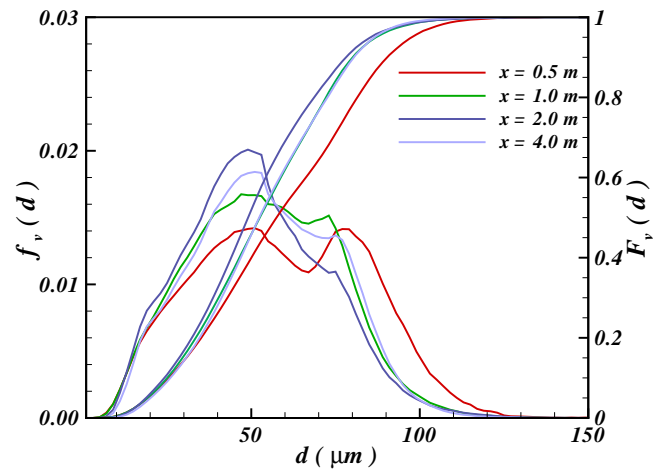


**FIGURE 18.** VOLUMETRIC PROBABILITY DENSITY FUNCTIONS,  $f_v(d)$ , AND CUMULATIVE DISTRIBUTIONS,  $F_v(d)$ , BASED ON TEMPORAL SAMPLES OF THE DATA OBTAINED USING PDI.

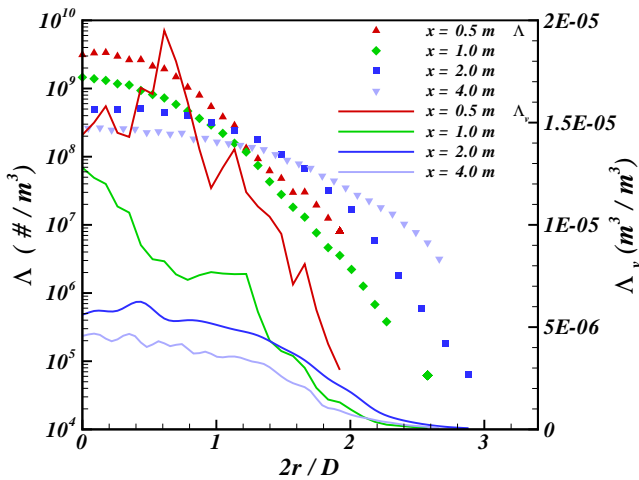


**FIGURE 17.** RADIAL PROFILES OF NUMBER CONCENTRATION,  $\Lambda$ , REPRESENTED BY SYMBOLS AND VOLUME CONCENTRATION,  $\Lambda_v$ , REPRESENTED BY SOLID LINES AT VARIOUS STREAMWISE POSITIONS. CONCENTRATION OBTAINED FROM PDI DATA BY TRANSFORMATION.

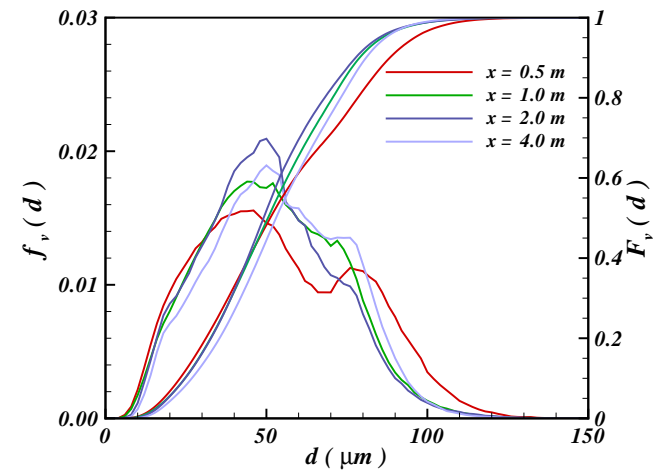


**FIGURE 19.** VOLUMETRIC PROBABILITY DENSITY FUNCTIONS,  $f_v(d)$ , AND CUMULATIVE DISTRIBUTIONS,  $F_v(d)$ , BASED ON SPATIAL SAMPLES OBTAINED FROM PDI DATA BY TRANSFORMATION.

The PDI data results transformed to spatial samples (Fig. 19) may be compared directly to the LD data shown in Fig. 7. This has been shown for the data at  $x=4.0\text{ m}$  in Fig. 20 and the correspondence is very good at this position. In the near wake, where the spray is highly non-uniform and unsteady, the correspondence is poor.

## SUMMARY

Comparison of the LD and transformed PDI results at a distance of  $4.0\text{ m}$  downstream of the atomizer showed some similarities but in the near wake,  $x < 1.0\text{ m}$ , the results were qualitatively different. In particular, the number of large droplets recorded by PDI was greater than with LD. Some possible reasons for this difference are as follows:

1. Multiple Scattering in LD: This situation occurs when [23]:



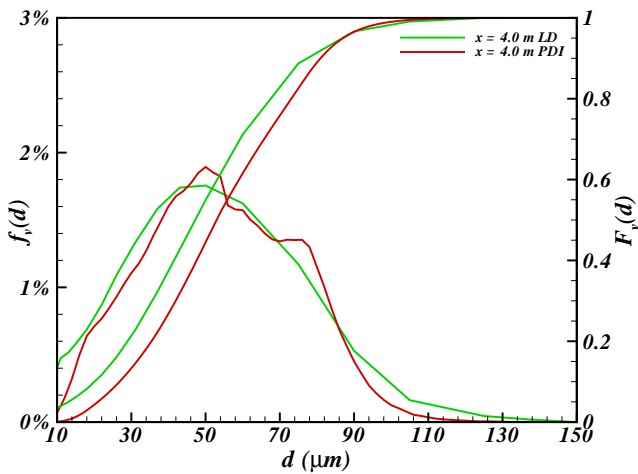


**FIGURE 20.**  $f_v(d)$  AND  $F_v(d)$  BASED ON SPATIAL SAMPLES OBTAINED FROM PDI DATA BY TRANSFORMATION AND LD SYSTEM AT  $x=4.0$  m.

a- the droplet number concentration is high and the small interparticle spacing causes the dependence of the scattering pattern of a single droplet on the size and position of the adjacent droplets, b- where the probability of finding a droplet in the optical path of another droplet is high. In the literature [24] it has been noted that when the obscuration is higher than  $\sim 60\%$  the effect of multiple scattering becomes significant on the calculated size distribution of the droplets. Multiple scattering usually results in a decrease in the average droplet diameter [24]. In the present study high values of obscuration and droplet concentration at the center of plume, see Figs. 4&17, demands a close investigation of the effects of multiple scattering on the results.

2. Signal Rejection in PDI: The high data rate of the small droplets at the center of the plume at  $x=0.5$  m caused the rejection of 40% of the detected signals. At each point the number of rejected droplet is correlated to the number rate of droplets in each droplet size bin. This does not affect single point statistics such as  $d_{v,0.5}$  but can affect the number and volume fraction of each size class in the aggregated data. The number of rejections can be reduced with more careful control of aperture size or by using lower liquid flow rates.
3. Transforming between Temporal and Spatial Samples: In order to transform the temporal PDI sample to the spatial sample a mean velocity of each size class in x direction is used. This method can be made more accurate if all 3 components of the velocity are used and this is possible with the current instrument. A more severe limitation of the transform is its restriction to low turbulence levels whereas in the near wake

## References

- [1] ASTM E799 - 03 standard practice for determining data criteria and processing for liquid drop size analysis.
- [2] MICRON SPRAYERS LIMITED. *AU4000 ATOMISER Operator's Handbook and Parts Catalogue*.
- [3] van Vliet, M., and Picot, J., 1987. "Drop spectrum characterization for the micronair AU4000 aerial spray atomizer". *Atomisation and Spray Technology*, **3**, pp. 123–134.
- [4] Parkin, C., and Siddiqui, H., 1990. "Measurement of drop spectra from rotary cage aerial atomizers". *Crop Protection*, **9**(1), pp. 33–38.
- [5] Teske, M. E., Thistle, H. W., Hewitt, A. J., Kirk, I. W., Dexter, R. W., and Ghent, J. H., 2005. "Rotary atomizer drop size distribution database". *Transactions of the American Society of Agricultural Engineers*, **48**, pp. 917–921.
- [6] Hewitt, A. J., 2002. Sampling techniques for droplet sizing of rotary atomizer sprays. Tech. rep., SERG International.
- [7] Hewitt, A. J., Robinson, A. G., Sanderson, R., and Huddleston, E. W., 1994. "Comparison of the droplet size spectra produced by rotary atomizers and hydraulic nozzles under simulated aerial application conditions". *Journal of Environmental Science and Health, Part B*, **29**(4), pp. 647–660.
- [8] Dodge, L. G., 1988. "Representation of average drop sizes in sprays". *Journal of Propulsion and Power*, **4**, pp. 490–496.
- [9] Dodge, L. G., Rhodes, D. J., and Reitz, R. D., 1987. "Drop-size measurement techniques for sprays: comparison of malvern laser-diffraction and aerometrics phase/doppler". *Applied Optics*, **26**, pp. 2144–54.
- [10] Chapple, A., Taylor, R., and Hall, F., 1995. "The transformation of spatially determined drop sizes to their temporal equivalents for agricultural sprays". *Journal of Agricultural Engineering Research*, **60**(1), pp. 49–56.
- [11] Herbst, A., 2001. "Droplet sizing on agricultural sprays—a comparison of measuring systems using a standard droplet size classification scheme". *Proceedings Ilass Europe 2001*.
- [12] Hoffmann, W. C., Hewitt, A., Ross, J., Bagley, W., Martin, D., and Fritz, B., 2008. "Spray adjuvant effects on droplet size spectra measured by three laser-based systems in a high-speed wind tunnel". *Journal of ASTM international*, **5**(6), pp. 60–71.
- [13] Albrecht, H.-E., Borys, M., Damasche, N., and Tropea, C., 2003. *Laser doppler and phase doppler measurement techniques*. Springer, Berlin ; New York.
- [14] Chuang, P. Y., Saw, E. W., Small, J. D., Shaw, R. A., Sipperley, C. M., Payne, G. A., and Bachalo, W. D., 2008. "Airborne phase doppler interferometry for cloud microphysical measurements". *Aerosol Science and Technology*, **42**, pp. 685–703.
- [15] Widmann, J. F., Presser, C., and Leigh, S. D., 2001. "Improving phase doppler volume flux measurements in low

- data rate applications”. *Measurement Science & Technology*, **12**, pp. 1180–90.
- [16] Nuyttens, D., Baetens, K., Schampheleire, M. D., and Sonck, B., 2007. “Effect of nozzle type, size and pressure on spray droplet characteristics”. *Biosystems Engineering*, **97**, pp. 333–345.
- [17] Chen, Z., Li, Z., Wang, F., Jing, J., Chen, L., and Wu, S., 2008. “Gas/particle flow characteristics of a centrally fuel rich swirl coal combustion burner”. *Fuel*, **87**, pp. 2102–2110.
- [18] Young, B., and Bachalo, W., 1987. “The direct comparison of three in-flight droplet sizing techniques for pesticide spray research”. In International Symposium on optical particle sizing: theory and practice.
- [19] Crowe, C. T., Sommerfeld, M., and Tsuji, Y., 1998. *Multiphase flows with droplets and particles*. CRC Press, Boca Raton, FL.
- [20] Bachalo, W., 1980. “Method for measuring the size and velocity of spheres by dual-beam light-scatter interferometry”. *Applied Optics*, **19**, pp. 363 – 70.
- [21] Bachalo, W., and Houser, M., 1984. “Phase/Doppler spray analyzer for simultaneous measurements of drop size and velocity distributions”. *Optical Engineering*, **23**, pp. 583–590.
- [22] Roisman, I. V., and Tropea, C., 2001. “Flux measurements in sprays using phase doppler techniques”. *Atomization and Sprays*, **11**(6), pp. 667–699.
- [23] Hirleman, E., 1988. “Modeling of multiple scattering effects in Fraunhofer diffraction particle size analysis”. *Particle & Particle Systems Characterization*, **5**(2), pp. 57–65.
- [24] Dumouchel, C., Yongyingsakthavorn, P., and Cousin, J., 2009. “Light multiple scattering correction of laser-diffraction spray drop-size distribution measurements”. *International Journal of Multiphase Flow*, **35**(3), pp. 277–287.